

Far-infrared ellipsometric study of the spectral gap in the c -axis conductivity of $Y_{1-x}Ca_xBa_2Cu_3O_{7-\delta}$ crystals

C. Bernhard, D. Munzar,* A. Wittlin,† W. König, A. Golnik,‡ and C. T. Lin
Max-Planck-Institut für Festkörperforschung, D-70569 Stuttgart, Germany

M. Kläser
Kristall- und Materiallabor, Universität Karlsruhe, D-76128 Karlsruhe, Germany

Th. Wolf
Forschungszentrum Karlsruhe, Institut für Theoretische Physik, D-76021 Karlsruhe, Germany

G. Müller-Vogt
Kristall- und Materiallabor, Universität Karlsruhe, D-76128 Karlsruhe, Germany

M. Cardona
Max-Planck-Institut für Festkörperforschung, D-70569 Stuttgart, Germany

(Received 11 December 1998)

The temperature (T) and doping dependence of the spectral gap in the far-infrared c -axis conductivity of $Y_{1-x}Ca_xBa_2Cu_3O_{7-\delta}$ has been studied by ellipsometry. For underdoped crystals a T -independent spectral gap is observed which persists almost unchanged into the normal state. The normal-state gap disappears at optimum doping whereas a conventional T dependence of the spectral gap is found for overdoped samples. The analogy to the results of angle-resolved photoemission suggests that the c -axis conductivity may be dominated by the carriers at the X point of the two-dimensional Brillouin zone. [S0163-1829(99)50910-7]

It is widely recognized that the normal-state (NS) gap in the low-energy spin and charge excitations of the CuO_2 planes may be central to the understanding of high- T_c superconductivity in the cuprates. The NS gap was originally observed in NMR experiments and viewed as a “spin gap.”¹ Recently, specific-heat and magnetic-susceptibility measurements² have shown that the NS gap also involves the charge excitations. This finding has been reinforced by angle-resolved photoemission spectroscopy (ARPES) (Refs. 3–5) and tunneling experiments.⁶ The signatures of the NS gap have also been identified in optical studies.^{7–9} In particular, a gaplike suppression of the NS far-infrared (FIR) c -axis conductivity was observed in underdoped $YBa_2Cu_3O_{7-\delta}$ (Y-123) (Refs. 7 and 9) and $YBa_2Cu_4O_8$.¹⁰

In order to explain the NS gap a vast number of models have been proposed which are based on different mechanisms, such as short-range superconducting (SC) fluctuations,¹¹ spinon pairing in Luttinger-liquid models,¹² or a precursor of an antiferromagnetic spin-density wave state,¹³ just to mention a few. However, the origin of the NS gap is still unclear. It is even debated whether the various experimental techniques probe a unique NS gap effect.

In this paper we report on ellipsometric measurements of the FIR c -axis conductivity of $Y_{1-x}Ca_xBa_2Cu_3O_{7-\delta}$ (Y,Ca-123) crystals which show in detail how the spectral gap develops as a function of T and hole doping ranging from underdoped to overdoped. The preparation of Y,Ca-123 crystals has been described elsewhere.¹⁴ The midpoint transition temperature T_c and the transition width ΔT_c (10–90%) have been determined with a superconducting quantum interference device (SQUID) magnetometer.

The ellipsometric measurements have been performed at the U4IR beamline of the National Synchrotron Light Source (NSLS) at Brookhaven National Laboratory, using a home-built setup attached to a Nicolet Fast-Fourier Spectrometer.¹⁵ The technique of ellipsometry¹⁵ provides significant advantages over conventional reflection methods in that (i) it is self-normalizing and does not require reference measurements, and (ii) the real and the imaginary parts of the dielectric function, $\epsilon = \epsilon_1 + i\epsilon_2$, are obtained directly without a Kramers-Kronig transformation. In combination with the high brilliance of the synchrotron this enables us to perform very accurate measurements of ϵ on crystals with ac faces as small as $0.5 \times 1 \text{ mm}^2$. Since only relative intensities are required, the ellipsometric measurements are very reproducible and the data taken at a given T before and after thermal cycling, or several days of measurements, coincide to within the noise level. In particular, this allows us to resolve very small changes of ϵ with T and doping. Note that the data presented in this paper are obtained from the pseudodielectric functions measured with the c axis along the line of intersection between the plane of incidence and the sample surface. It was shown previously that the fit obtained using the full anisotropic tensor elements did not alter the results.¹⁵

Figure 1(a) shows the real part of the c -axis conductivity, σ_{1c} , for an underdoped $YBa_2Cu_3O_{6.75}$ crystal with $T_c = 78(2) \text{ K}$. Superimposed on the electronic (el.) background are the seven IR-active phonon modes at 155, 190, 285, 320, 570, 620, and 630 cm^{-1} .^{7–9} In addition, at low T a broad peak (whose origin is not yet understood) forms around 500 cm^{-1} at the expense of the phonons at 320 cm^{-1} and 570 cm^{-1} .^{7,9} The contributions of the phonons and the broad

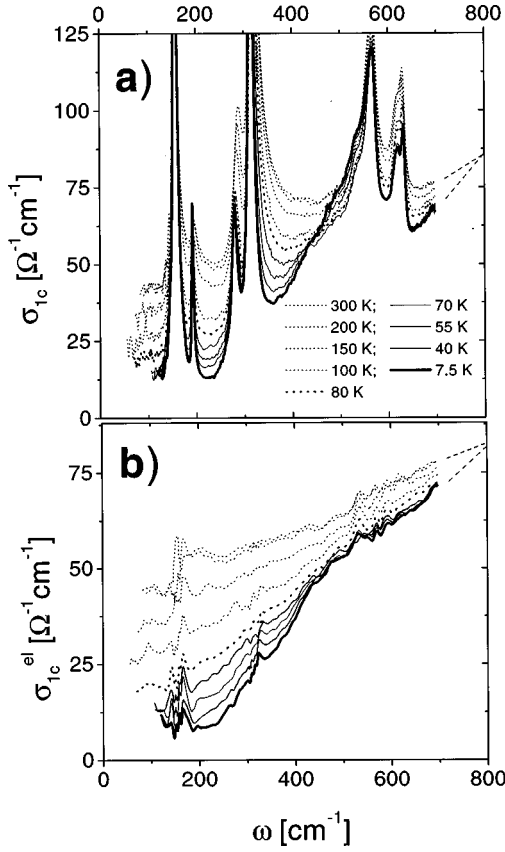


FIG. 1. (a) The c -axis conductivity, σ_{1c} , of underdoped $\text{YBa}_2\text{Cu}_3\text{O}_{6.75}$. The dashed lines indicate the extrapolation beyond the measured spectral range. (b) The el. conductivity, σ_{1c}^{el} , which is obtained after the contributions of the seven phonons and the broad peak around 500 cm^{-1} have been subtracted.

peak have been obtained by fitting a sum of modified Lorentzian functions, $\varepsilon(\omega) = S\omega_0^2 \exp(i\Phi)/[(\omega_0^2 - \omega^2) - i\omega\Gamma]$,^{7,9} to the complex dielectric function. Details will be reported elsewhere.¹⁶ Figure 1(b) displays the el. conductivity, σ_{1c}^{el} , which has been obtained by subtracting the contributions of the phonons and the broad peak from σ_{1c} . Note that the phonon subtraction does not strongly affect the general features of the electronic background in the relevant high frequency region. At the lowest T reached ($T=7.5 \text{ K}$), σ_{1c}^{el} can be seen to decrease almost linearly towards zero frequency while remaining finite up to the lowest measured frequencies. This behavior has been previously reported and explained in terms of the unconventional d -wave symmetry of the SC order parameter for which quasiparticles can be excited across the gap nodes for any finite photon energy.^{7,9} Here we concentrate on the spectral gap which manifests itself as a suppression of σ_{1c}^{el} with decreasing temperature. We define the size of the spectral gap as the frequency of the onset of this suppression. In the SC state its size (as estimated with respect to σ_{1c}^{el} at $T \sim T_c$) roughly corresponds to 2Δ , where Δ is the maximum value of the d -wave-SC gap.¹⁷ From Fig. 1 it appears that 2Δ is above the upper limit of the measured spectral range: by extrapolation (dashed lines) we obtain $2\Delta(T \rightarrow 0) = 800(30) \text{ cm}^{-1}$. Most notably, the el. conductivity in the high frequency region remains almost T independent in the SC state. This implies that 2Δ does not decrease with increasing T . In the SC state σ_{1c}^{el} increases

with T only at frequencies well below 2Δ . The overall T dependence of σ_{1c}^{el} is indicative of a strongly anisotropic and T -independent-SC gap which merely fills in with thermally excited quasiparticles from the gap nodes.¹⁷ It can be seen that the spectral gap persists in the NS far beyond T_c . Notably, the NS spectral gap has a very similar size and shape like the SC gap and does not seem to decrease with increasing T . The increase of σ_{1c}^{el} at high frequencies seems rather to be related to a filling in of the gap which is completed at a certain temperature, $T^* \sim 200 \text{ K}$, above which σ_{1c}^{el} becomes almost T and ω independent.

We note that results strikingly similar to those reported above have been obtained in ARPES studies³⁻⁵ on $\text{Bi}_2\text{Sr}_2\text{CaCu}_2\text{O}_{8+\delta}$ (Bi-2212) which probe the in-plane spectral function. The ARPES spectra around the X point of the two-dimensional (2D) Brillouin-zone (BZ) reveal a gap of T -independent magnitude which persists almost unchanged in the NS.^{3,5} The NS gap does not decrease in size with increasing T but merely fills in (the pit in the spectral function is getting shallower) and the spectral function becomes nearly flat above a specific temperature, T^* . We note that there is growing experimental evidence that the electronic properties of the cuprate compounds are determined mainly by the CuO_2 planes (see, e.g., Ref. 19). We therefore assume that it is possible to correlate the ARPES data on Bi-2212 and the c -axis conductivity of Y-123 and suggest—on the grounds of the analysis mentioned above—that the spectral features of the c -axis conductivity are determined by the el. structure around the X point. The contribution from the regions around the BZ diagonal, where the NS gap in the ARPES spectra closes rapidly and a well-defined quasiparticle peak occurs,⁵ appears to be less important. This idea is consistent with band-structure calculations¹⁸ which predict strongly anisotropic intra- and interbilayer c -axis hopping rates, which are largest at the X point and vanish along the BZ diagonal. The c -axis transport may be incoherent (not conserving momentum), especially in the underdoped case. Nevertheless, the interlayer scattering matrix elements¹⁷ are likely to be strongly influenced by the anisotropy of the one-electron hopping rates mentioned above. Following these ideas, we have calculated the contribution $\sigma(k_F, \omega, T)$ of a k -point k_F located at the Fermi crossing along $(\pi/a, 0) - (\pi/a, \pi/a)$ (close to X) to the conductivity, using the spectral function $A(k_F, \omega, T)$ presented in Ref. 5:

$$\sigma(k_F, \omega, T) \sim \int d\omega' A(k_F, \omega', T) A(k_F, \omega + \omega', T) \times \frac{n_F(\omega', T) - n_F(\omega + \omega', T)}{\omega}.$$

The latter spectral function was obtained from the ARPES data of underdoped Bi-2212 with $T_c = 83 \text{ K} < T_{c, \text{max}} = 92 \text{ K}$,⁵ close to $T_c = 78 \text{ K} < T_{c, \text{max}} = 92 \text{ K}$ of our Y-123 sample. The results shown in Fig. 2 reproduce the main features of our experimental spectra of Fig. 1(b).

The similarity between the NS and the SC gap at the X point has led to the suggestion that the NS gap is related to a precursor SC state.^{3,5} Our data, however, do not support such a scenario since we find that the missing spectral weight related to the NS gap does not contribute to the SC delta

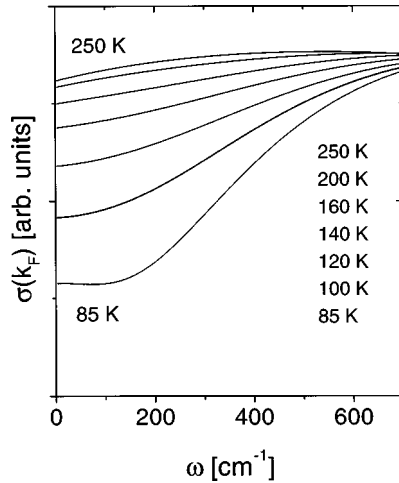


FIG. 2. Contribution of a k -point k_F at the $(\pi/a, 0)$ - $(\pi/a, \pi/a)$ Fermi crossing (close to X) to the conductivity calculated from the ARPES spectral function of Ref. 5.

function at zero frequency once a coherent SC state is established below T_c . Instead, it is shifted towards higher frequencies beyond the range covered by our experiment. Direct evidence for such a shift has been obtained from reflectivity measurements which cover a wider frequency range.¹⁰ We have determined the unscreened plasma frequency of the superconducting condensate from the zero crossing of ϵ_1^{el} (with the phonons subtracted) at 205 cm^{-1} to be $\omega_{ps} \approx (205 \text{ cm}^{-1} / \sqrt{\epsilon_\infty}) = 420 \text{ cm}^{-1}$, where $\epsilon_\infty = 4.2$ was adopted from Ref. 8. Details of the procedure will be presented elsewhere.¹⁶ According to the sum rule, we should obtain $\omega_{ps}^2 = (120/\pi) \int_0^{700} [\sigma_{1c}(\omega, 300 \text{ K}) - \sigma_{1c}(\omega, 7.5 \text{ K})] d\omega$ if the NS gap was related to a precursor SC state, whereas $\omega_{ps}^2 = (120/\pi) \int_0^{700} [\sigma_{1c}(\omega, 80 \text{ K}) - \sigma_{1c}(\omega, 7.5 \text{ K})] d\omega$ should hold otherwise. For the estimate of the missing area, we extrapolated the conductivity towards zero frequency values of $\sigma_{1c}(\omega=0)$ of $40 \text{ } \Omega^{-1} \text{ cm}^{-1}$ at 300 K, $14 \text{ } \Omega^{-1} \text{ cm}^{-1}$ at 80 K, and $0 \text{ } \Omega^{-1} \text{ cm}^{-1}$ at 7.5 K. We obtain $\omega_{ps}(\text{SC+NS gap}) \approx 750 \text{ cm}^{-1}$ and $\omega_{ps}(\text{SC gap}) \approx 450 \text{ cm}^{-1}$.

Despite this rather crude estimate, the difference between the two cases seems to be significant and suggests that the NS gap is not related to a precursor SC state. This finding implies that the SC and the NS gaps compete for the available spectral weight.² Nevertheless, it is yet unclear whether the SC and the NS gaps have a different or a common origin.^{2,12,13}

Next we turn to the changes of the spectral gap with increasing hole doping. Figures 3(a)–3(f) show σ_{1c} and σ_{1c}^{el} for three $\text{Y}_{0.86}\text{Ca}_{0.14}\text{Ba}_2\text{Cu}_3\text{O}_{7-\delta}$ crystals with different oxygen content: (a) slightly underdoped with $\delta=0.4$ and $T_c = 83(4) \text{ K}$; (b) optimally doped with $\delta=0.3$ and $T_c = 86(3) \text{ K}$; and (c) strongly overdoped with $\delta=0.1$ and $T_c = 75(3) \text{ K}$. Figures 3(a) and 3(b) show that the signature of the NS gap (i.e., the suppression of σ_{1c}^{el} with decreasing T) still is evident for the crystal which is only slightly underdoped. Apart from the slightly reduced gap size of $2\Delta \approx 700(20) \text{ cm}^{-1}$ (as indicated by the solid arrow), the spectral features are similar to those of the underdoped Y-123 crystal (Fig. 1). For the optimally-doped crystal, even though it is only slightly more oxygenated, the NS gap is absent. The spectral gap fills in around T_c and the electronic c -axis conductivity remains almost T and ω independent in the normal state [Figs. 3(c) and 3(d), see also Ref. 19], i.e., $T_c \approx T^*$. The gap size is again slightly reduced to $2\Delta \approx 650(20) \text{ cm}^{-1}$. Finally, Figs. 3(e) and 3(f) display σ_{1c} and σ_{1c}^{el} for the overdoped crystal. The data are shown only for the SC state and slightly above T_c . Additional NS data well above T_c have been omitted for clarity but σ_{1c} was previously shown to exhibit a metallic behavior in that case.¹⁹ The size of the spectral gap is once more considerably reduced to $2\Delta \approx 530(20) \text{ cm}^{-1}$. This confirms the previous reports from ARPES and tunneling experiments that the gap size decreases towards the overdoped regime^{4,5} while it increases on the underdoped side^{3,5,6} despite the decrease in T_c . Another remarkable feature of the overdoped sample is the large fraction, of quasiparticles which remain unpaired and fill in the spectral gap. Apparently, this Drude component which is absent in the underdoped crystals, grows rapidly on the overdoped side. The origin of these carriers is yet unclear but seems to be related to the suppression of the NS gap.¹⁹ Since

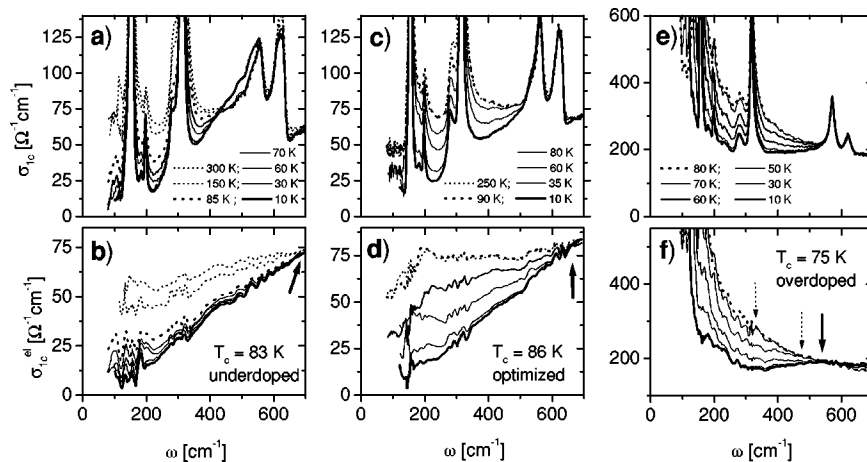


FIG. 3. The c -axis conductivity, σ_{1c} , and the el. background, σ_{1c}^{el} , of three $\text{Y}_{0.86}\text{Ca}_{0.14}\text{Ba}_2\text{Cu}_3\text{O}_{7-\delta}$ crystals: (a,b) underdoped with $\delta \approx 0.4$ and $T_c = 83 \text{ K}$, (c,d) optimally doped with $\delta \approx 0.3$ and $T_c = 86 \text{ K}$, and (e,f) overdoped with $\delta \approx 0.15$ and $T_c = 75 \text{ K}$. The arrows indicate the onset of the spectral gap.

their contribution is more pronounced in the c -axis conductivity than in the in-plane optical response²⁰ and the specific heat² of similarly overdoped samples, we speculate that these unpaired carriers may originate mainly from a k -space region close to the X point (cf. our arguments given above). We note that the predominant appearance of the unpaired carriers in σ_{1c} cannot be easily explained by impurity scattering which should be most efficient at the gap nodes. In fact, it is known that Zn substitution causes strong pair breaking and indeed the resulting unpaired carriers show up clearly in the in-plane optical response but hardly in the c -axis response.²¹ Finally, we comment on the T dependence of the SC gap in the overdoped crystal. It is evident from Fig. 3(f) that the gap exhibits a rather conventional T dependence, i.e., it decreases with increasing T (the onset of the missing area is reduced to $\sim 480 \text{ cm}^{-1}$ at 60 K and to $\sim 300 \text{ cm}^{-1}$ at 70 K) and it closes at T_c . This conventional T dependence contrasts with the T -independent gap size of the underdoped crystals. We emphasize that a corresponding trend has been obtained in ARPES studies on overdoped Bi-2212.^{4,5}

In summary, the T and doping dependence of the spectral gap in the FIR c -axis conductivity of Y,Ca-123 crystals has

been studied by ellipsometric measurements which are more accurate and precise than conventional reflection measurements. We show that on the underdoped side the spectral gap is T independent and persists almost unchanged in the NS having a similar size and shape like the SC gap. The NS gap, however, cannot be related to a precursor SC state since it depletes the SC condensate which forms below T_c . We show that the NS spectral gap disappears at optimum doping and that the SC spectral gap of overdoped samples exhibits a rather conventional T dependence and closes at T_c . The gap size is found to decrease continuously with increasing hole doping. Many aspects of our spectra and, in particular, a comparison between the spectra of the underdoped samples and an estimate based on ARPES data suggest that the c -axis conductivity is dominated by the carriers around the X point of the two-dimensional BZ.

We thank D. Böhme for technical help and G. P. Williams and L. Carr for support at the U4IR beamline of the NSLS. We acknowledge E. Brücher and R. Kremer for SQUID measurements. D.M. was supported by the AvH foundation. A.W. acknowledges the KBN GRANT No. 2P03B7011.

*Permanent address: Department of Solid State Physics, Faculty of Science, Masaryk University, Kotlářská 2, 61137 Brno, Czech Republic.

†Permanent address: Inst. of Physics, P.A.S., Al. Lotników 32, 02-668 Warsaw, Poland.

‡Permanent address: IFD, Warsaw University, Hoża, 69, 00-681 Warsaw, Poland.

¹H. Alloul, T. Ohno, and P. Mendels, *Phys. Rev. Lett.* **63**, 1700 (1989).

²J. W. Loram *et al.*, *Phys. Rev. Lett.* **71**, 1740 (1993); *Physica C* **282-287**, 1405 (1997).

³A. G. Loeser *et al.*, *Science* **273**, 325 (1996); H. Ding *et al.*, *Nature (London)* **382**, 51 (1996).

⁴P. J. White *et al.*, *Phys. Rev. B* **54**, 15 669 (1996).

⁵N. Norman *et al.*, *Phys. Rev. B* **57**, 11 093 (1998); *Nature (London)* **392**, 157 (1998).

⁶N. Miyakawa *et al.*, *Phys. Rev. Lett.* **80**, 157 (1998); Ch. Renner *et al.*, *ibid.* **80**, 149 (1998).

⁷C. C. Homes *et al.*, *Phys. Rev. Lett.* **71**, 1645 (1993); *Physica C* **254**, 265 (1995).

⁸A. P. Litvinchuk, C. Thomsen, and M. Cardona, in *Physical Properties of HTSC*, edited by D. M. Ginsberg (World Scientific, Singapore, 1994), Vol. IV, p. 375.

⁹J. Schützmann *et al.*, *Phys. Rev. B* **52**, 13 665 (1995); S. Tajima *et al.*, *ibid.* **55**, 6051 (1997).

¹⁰D. N. Basov *et al.*, *Phys. Rev. B* **52**, 13 141 (1995); **50**, 3511 (1994).

¹¹V. J. Emery and S. A. Kivelson, *Nature (London)* **374**, 434 (1995).

¹²P. W. Anderson, *J. Phys.: Condens. Matter* **8**, 10 083 (1996); P. A. Lee and X. G. Wen, *Phys. Rev. Lett.* **76**, 503 (1996).

¹³A. V. Chubukov and J. Schmalian, *Phys. Rev. B* **57**, R11 085 (1998), and references therein.

¹⁴T. Zenner *et al.*, *J. Low Temp. Phys.* **105**, 909 (1996).

¹⁵J. Kircher *et al.*, *J. Opt. Soc. Am. B* **14**, 705 (1997); R. Henn *et al.*, *Thin Solid Films* **313-314**, 643 (1998); R. Henn, Ph.D. thesis, University of Stuttgart, 1997.

¹⁶C. Bernhard *et al.* (unpublished).

¹⁷This is almost exact in the “dirty limit.” See P. J. Hirschfeld *et al.*, *Phys. Rev. B* **55**, 12 742 (1997); M. Palumbo and M. J. Graf, *ibid.* **53**, 2261 (1996).

¹⁸O. K. Andersen *et al.*, *J. Phys. Chem. Solids* **56**, 1573 (1995); T. Xiang and J. M. Wheatley, *Phys. Rev. Lett.* **77**, 4632 (1996).

¹⁹C. Bernhard *et al.*, *Phys. Rev. Lett.* **80**, 1762 (1998).

²⁰M. Prenninger *et al.*, *Physica C* **235-240**, 1131 (1994).

²¹N. L. Wang *et al.*, *Phys. Rev. B* **57**, R11 081 (1998).